Astronomy & Astrophysics

Planck intermediate results

XVI. Profile likelihoods for cosmological parameters

Planck Collaboration: P. A. R. Ade[79], N. Aghanim[56], M. Arnaud[68], M. Ashdown[65,6], J. Aumont[56], C. Baccigalupi[77], A. J. Banday[81,10],
R. B. Barreiro[62], J. G. Bartlett[1,63], E. Battaner[82,83], K. Benabed[57,80], A. Benoit-Lévy[21,57,80], J.-P. Bernard[81,10], M. Bersanelli[33,48],
P. Bielewicz[81,10,77], J. Bobin[68], A. Bonaldi[64], J. R. Bond[9], F. R. Bouchet[57,80], C. Burigana[47,31], J.-F. Cardoso[69,1,57], A. Catalano[70,67],
A. Chamballu[68,15,56], H. C. Chiang[25,7], P. R. Christensen[75,36], D. L. Clements[53], S. Colombi[57,80], L. P. L. Colombo[20,63], F. Couchot[66], F. Cuttaia[47],
L. Danese[77], R. D. Davies[64], R. J. Davis[64], P. de Bernardis[32], A. de Rosa[47], G. de Zotti[43,77], J. Delabrouille[1], C. Dickinson[64], J. M. Diego[62],
H. Dole[56,55], S. Donzelli[48], O. Doré[63,11], M. Douspis[56], X. Dupac[39], T. A. Enßlin[73], H. K. Eriksen[60], F. Finelli[47,49], O. Forni[81,10], M. Frailis[45],
E. Franceschi[47], S. Galeotta[45], S. Galli[57], K. Ganga[1], M. Giard[81,10], Y. Giraud-Héraud[1], J. González-Nuevo[62,77], K. M. Górski[63,84],
A. Gregorio[34,45,51], A. Gruppuso[47], F. K. Hansen[60], D. L. Harrison[59,65], S. Henrot-Versillé[66], C. Hernández-Monteagudo[12,73], D. Herranz[62],
S. R. Hildebrandt[11], E. Hivon[57,80], M. Hobson[6], W. A. Holmes[63], A. Hornstrup[16], W. Hovest[73], K. M. Huffenberger[23], A. H. Jaffe[53],
T. R. Jaffe[81,10], W. C. Jones[25], M. Juvela[24], E. Keihänen[24], R. Keskitalo[13], T. S. Kisner[72], R. Kneissl[38,8], J. Knoche[73], L. Knox[27], M. Kunz[17,56,3],
H. Kurki-Suonio[24,41], G. Lagache[56], A. Lähteenmäki[2,41], J.-M. Lamarre[67], A. Lasenby[6,65], C. R. Lawrence[63], R. Leonardi[39], A. Liddle[78,22],
M. Liguori[30], P. B. Lilje[60], M. Linden-Vørnle[16], M. López-Caniego[62], P. M. Lubin[28], J. F. Macías-Pérez[70], B. Maffei[64], D. Maino[33,48],
N. Mandolesi[47,5,31], M. Maris[45], P. G. Martin[9], E. Martínez-González[62], S. Masi[32], S. Massardi[46], S. Matarrese[30], P. Mazzotta[35],
A. Melchiorri[32,50], L. Mendes[39], A. Mennella[33,48], M. Migliaccio[59,65], S. Mitra[52,63], M.-A. Miville-Deschênes[56,9], A. Moneti[57], L. Montier[81,10],
G. Morgante[47], D. Munshi[79], J. A. Murphy[74], P. Naselsky[75,36], F. Nati[32], P. Natoli[31,4,47], F. Noviello[64], D. Novikov[53], I. Novikov[75],
C. A. Oxborrow[16], L. Pagano[32,50], F. Pajot[56], D. Paoletti[47,49], F. Pasian[45], O. Perdereau[66], L. Perotto[70], F. Perrotta[77], V. Pettorino[17], F. Piacentini[32],
M. Piat[1], E. Pierpaoli[20], D. Pietrobon[63], S. Plaszczynski[66,*], E. Pointecouteau[81,10], G. Polenta[4,44], L. Popa[58], G. W. Pratt[68], J.-L. Puget[56],
J. P. Rachen[19,73], R. Rebolo[61,14,37], M. Reinecke[73], M. Remazeilles[64,56,1], C. Renault[70], S. Ricciardi[47], T. Riller[73], I. Ristorcelli[81,10], G. Rocha[63,11],
C. Rosset[1], G. Roudier[1,67,63], B. Rouillé d'Orfeuil[66], J. A. Rubiño-Martín[61,37], B. Rusholme[54], M. Sandri[47], M. Savelainen[24,41], G. Savini[76],
L. D. Spencer[79], M. Spinelli[66], J.-L. Starck[68], F. Sureau[68], D. Sutton[59,65], A.-S. Suur-Uski[24,41], J.-F. Sygnet[57], J. A. Tauber[40], L. Terenzi[47],
L. Toffolatti[18,62], M. Tomasi[33,48], M. Tristram[66], M. Tucci[17,66], G. Umana[42], L. Valenziano[47], J. Valiviita[24,41], B. Van Tent[71], P. Vielva[62], F. Villa[47],
L. A. Wade[63], B. D. Wandelt[57,80,29], M. White[26], D. Yvon[15], A. Zacchei[45], and A. Zonca[28]

(Affiliations can be found after the references)

ABSTRACT

We explore the 2013 *Planck* likelihood function with a high-precision multi-dimensional minimizer (`Minuit`). This allows a refinement of the ΛCDM best-fit solution with respect to previously-released results, and the construction of frequentist confidence intervals using profile like-lihoods. The agreement with the cosmological results from the Bayesian framework is excellent, demonstrating the robustness of the *Planck* results to the statistical methodology. We investigate the inclusion of neutrino masses, where more significant differences may appear due to the non-Gaussian nature of the posterior mass distribution. By applying the Feldman-Cousins prescription, we again obtain results very similar to those of the Bayesian methodology. However, the profile-likelihood analysis of the cosmic microwave background (CMB) combination (*Planck*+WP+highL) reveals a minimum well within the unphysical negative-mass region. We show that inclusion of the *Planck* CMB-lensing information regularizes this issue, and provide a robust frequentist upper limit $\sum m_\nu \leq 0.26$ eV (95% confidence) from the CMB+lensing+BAO data combination.

Key words. cosmic background radiation – cosmology: observations – cosmology: theory – cosmological parameters – methods: statistical

1. Introduction

This paper, one of a set associated with the 2013 release of data from the *Planck*[1] mission (Planck Collaboration I 2014), de-scribes a frequentist estimation of cosmological parameters us-ing profile likelihoods.

Parameter estimation in cosmology is predominantly per-formed using Bayesian inference, particularly following the in-troduction of Markov chain Monte Carlo (MCMC) techniques (Christensen et al. 2001). Many scientists in the field use the sophisticated `CosmoMC`[2] software (Lewis & Bridle 2002) to study cosmological parameters, and several experiments pro-vide ready-to-use plugins for it. The *Planck* satellite mission has recently released high-quality data on the cosmic microwave background (CMB) temperature anisotropies[3]. The analysis of the cosmological parameters (Planck Collaboration XVI 2014) is based on Bayesian inference using a dedicated version of `CosmoMC`.

In this methodology, the likelihood leads to the posterior dis-tribution of the parameters once it has been multiplied by some prior distribution that encompasses our knowledge before the

---

[1] *Planck* (http://www.esa.int/Planck) is a project of the European Space Agency (ESA) with instruments provided by two sci-entific consortia funded by ESA member states (in particular the lead countries France and Italy), with contributions from NASA (USA) and telescope reflectors provided by a collaboration between ESA and a sci-entific consortium led and funded by Denmark.

[2] Available from http://cosmologist.info/cosmomc/readme_planck.html
[3] Available from http://www.sciops.esa.int/index.php?project=planck&page=Planck_Legacy_Archive

measurement is performed. For *Planck*, wide bounds on uniform distributions have typically been used. However the choice of a particular set of parameters for MCMC sampling, such as the efficient "physical basis" (Kosowsky et al. 2002) used in CosmoMC, may also be viewed as an implicit prior choice.

Frequentist methods do not need priors, other than that some limits on the explored domain are used in practice and can be seen as the bounds of some "uniform priors". The maximum likelihood estimate (MLE) does not depend on the choice of the set of parameters, since it possesses the property of invariance: if $\hat{\theta}$ represents the MLE of the parameter θ, then the MLE of any function $\tau(\theta)$ is $\hat{\tau} = \tau(\hat{\theta})$. This means that one can compute the MLE with any set of parameters. As we will see in Sect. 2.3, this property is powerful and can be used to obtain asymmetric confidence intervals.

The multi-dimensional solution is only one aspect of parameter estimation and we are also interested in statements on individual parameters. In the MCMC procedure, once the chains have converged this is obtained through marginalization, which is performed by a simple projection of the samples onto one or sometimes two axes. This may however lead to so-called "volume effects", where the mean of the projected distribution can become incompatible with the multi-dimensional MLE (e.g., Hamann et al. 2007). In the frequentist framework, one instead builds profile likelihoods (Wilks 1938) for individual variables and, by construction, the individual parameter estimates match (up to numerical accuracy) the MLE values.

Such a method has already been used by Yèche et al. (2006) with *Wilkinson* Microwave Anisotropy Probe (WMAP) data for a nine-parameter fit. The high sensitivity of data from *Planck* and from the ground-based South Pole Telescope (SPT) and Atacama Cosmology Telescope (ACT) projects requires the simultaneous fit of a larger number of parameters, up to about 40, with some nuisance ones being poorly constrained. We therefore need to precisely tune a high-quality minimizer, as will be described in this paper.

MCMC sampling is sometimes used to perform a "poorman's" determination of the maximum likelihood (e.g., Reid et al. 2010): one bins a given parameter and reports the sample of maximum likelihood in other dimensions. As pointed out in Hamann (2012), in many dimensions it is most likely that the real maximum was never reached in any reasonably-sized chain. The authors suggest changing the temperature of the chain, but this still requires running lengthy evaluations of the likelihood and is less straightforward than directly using a multi-dimensional minimization algorithm.

In this article, we investigate whether the use of priors or marginalization can affect the determination of the cosmological parameters by comparing the published Bayesian results to a frequentist method. For the base ΛCDM model, it happens that the cosmological parameter posteriors are essentially Gaussian, so it is expected that frequentist and Bayesian methods will lead to similar results. In extensions to the standard ΛCDM model this is however not true for some parameters (e.g., the sum of neutrino masses), and priors have been shown to play some role in parameter determination (Hamann et al. 2007; Gonzalez-Morales et al. 2011; Hamann 2012). Given the sensitivity of the *Planck* data, statistical methodologies may matter, and this issue is scrutinized in this work.

In order to build precise profile likelihoods in a high-dimensional space (up to about 40 dimensions), we need a powerful minimizer. We use the mature and widely-used Minuit software (James & Roos 1975). We interfaced it to the modular class Boltzmann solver (Blas et al. 2011) which, from a

set of input cosmological parameters, computes the corresponding temperature and polarization power spectra that are tested against the *Planck* likelihood. This required that we tune the class precision parameters to a level where the numerical noise can be handled by our minimizer, as is described in Sect. 2.1. In Sect. 2.2, we describe our Minuit minimization strategy, and cover in Sect. 2.3 the basics of the frequentist methodology to estimate unknown parameters based on the properties of profile likelihoods. The data sets we use are then discussed in Sect. 3. We give results for the ΛCDM parameters in Sect. 4.1 and finally investigate, in Sect. 4.2, a case where the posterior distribution is far from Gaussian, namely the neutrino mass case. Additionally, the Appendix gathers some comments on the overall computation time of the method.

2. Method

2.1. The Boltzmann solver: class

To compute the relevant CMB power spectra from a cosmological model, we need a "Boltzmann solver" that numerically evolves the coupled perturbation equations in an expanding universe. While camb is used in the CosmoMC sampler, we prefer to use the class (v1.6) software (Blas et al. 2011). It offers a rigorous way to control the accuracy of output quantities through a comprehensive list of precision parameters (Lesgourgues 2011a). While one can use some high-speed/low-quality settings to perform MCMC sampling because the random nature of the algorithm smooths out discontinuities, this is no longer the case here when searching for an extremum, which requires precise computation of numerical derivatives. Equally, due to computation time, one cannot use precision settings that are too extreme, so a trade-off with Minuit convergence has to be found.

As we will see in Sect. 2.3, 68% confidence intervals are obtained by cutting $\chi^2 \equiv -2 \ln \mathcal{L}$ values at one. We therefore need the numerical noise to be much less than unity.

Starting from the *Planck* likelihood code, described in Sect. 3, we fix all parameters to their published best-fit values (Planck Collaboration XVI 2014) and scan a given parameter θ. We compute the $\chi^2(\theta)$ curves and subtract a smooth component to estimate the amplitude of the numerical noise. According to the precision settings, trade-off between the amplitude of this noise and the computation time can then be found. An example with two precision settings is shown in Fig. 1 for $\theta = \omega_b = \Omega_b h^2$ which is used as our benchmark.

We have determined a set of high-precision settings which achieves sufficient smoothness of the *Planck* likelihood for the fits to converge, with an increase of only about a factor two in the code computation speed with respect to the default "fast" settings. The values of the settings are reported in Table 1.

We also found that working with the Thomson scattering optical depth τ is numerically less stable than using the reionization redshift z_{re}, which defines where the reionization fraction is half of its maximum. We therefore use z_{re} as a primary parameter. The relation to τ, for a tanh-based ionization profile and a fixed $\Delta z_{re} = 0.5$ width, is given in Lewis (2008).

Since we will compare our results to the previously-published ones, we need to ensure our class configuration reproduces the camb-based results of Planck Collaboration XVI (2014). For this purpose, we use the *Planck* ΛCDM best-fit solution and compute its χ^2 value and compare with the published results in Table 2. The agreement is good. The slight discrepancy is typical of the differences between class and camb
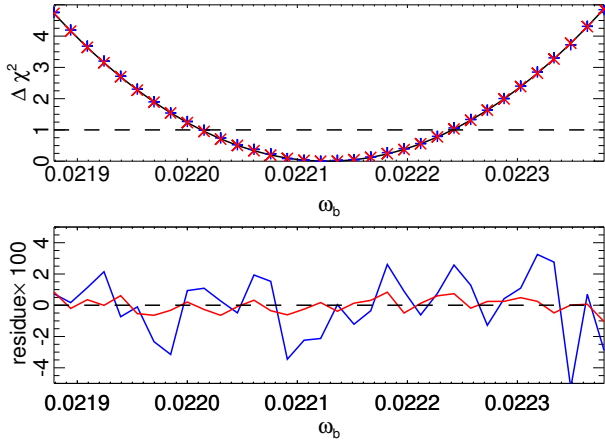
Fig. 1. *Upper panel*: the ω_b parameter is scanned (keeping all other parameters fixed to their best-fit values) and the *Planck* χ^2 values are shown on the vertical axis. Blue points are obtained with the `class` default settings, and red ones with our high-precision ones. A smooth parabola is fit and shown in black. *Lower panel*: residuals with respect to the parabola. The rms of this noise is improved from 0.02 for the default settings to 0.005 for the high-precision ones.

Table 1. Values of the non-default precision parameters for `class` used for the `Minuit` minimization.

`class` parameter	Value
tol_background_integration	10^{-3}
tol_thermo_integration	10^{-3}
tol_perturb_integration	10^{-6}
reionization_optical_depth_tol	10^{-5}
l_logstep	1.08
l_linstep	25
perturb_sampling_stepsize	0.04
delta_l_max	800

implementations (Lesgourgues 2011b), so we consider our setup to be properly calibrated. From now on, we perform consistent comparisons using only `class`.

2.2. Minimizing with `Minuit`

We chose to work with the powerful `Minuit` package (James & Roos 1975), a well-known minimizer originally developed for high-energy physics and used recently for the Higgs mass determination with a simultaneous fit of 354 parameters (ATLAS Collaboration 2013). While its roots trace back to the 1970s, it has been continually improved and rewritten in C++ as `Minuit2`, which is the version we use. `Minuit` is a toolbox including several algorithms that can be deployed depending on the problem under consideration. We refer the reader to the user guide[4] for a detailed description of the procedures we used.

For cosmological parameter estimation with the *Planck* data, we executed the following strategy

1. Starting from the Planck Collaboration published values and using the high-precision `class` settings described in Sect. 2.1, we minimize the χ^2 function using the `MIGRAD`

Table 2. Comparison of the χ^2 values of the *Planck* best-fit solution from Planck Collaboration XVI (2014), based on `camb`, to our `class`-based implementation, for the CMB and CMB+BAO data sets.

Data set	camb	class
CMB	10509.6	10509.9
CMB+BAO	10510.8	10511.0

algorithm, which is based on Fletcher's switching algorithm (Fletcher 1970). All parameters are bounded by large (or physical) limits during this exploration.

2. Once a minimum is found, we release all cosmological parameter limits and again perform the `MIGRAD` minimization. The limits on nuisance parameters are kept in order to avoid exploring unphysical regions.

3. Finally, we use the `HESSIAN` procedure which refines the local covariance matrix.

`MIGRAD` belongs to the category of variable metric methods (e.g., Davidon & Laboratory 1959) which build the "expected distance to minimum" (EDM) that represents (twice) the vertical distance to the χ^2 minimum if the function is truly quadratic and the gradient exactly known. It can serve as a figure of merit for the convergence and will be used to reject poor fits.

The outcome of this procedure is the minimum χ^2 solution together with its Hessian matrix. This solution represents the MLE, but, since the problem is highly non-linear (in particular in H_0), the Hessian is only a crude approximation to the parameter uncertainties[5]. The complete treatment is through the construction of profile likelihoods.

2.3. Profile likelihoods

The MLE (or "best-fit" or $\chi^2_{\rm min}$) is the global maximum likelihood estimate given the entire set of parameters (cosmological and nuisance). One can choose to isolate one parameter (hereafter called θ) and for fixed values of it look for the maximum of the likelihood function in all other dimensions. One scans θ within some range and, for each fixed value, runs a minimization with respect to all the other parameters. The minimum χ^2 value is reported for this parameter θ, which allows one to build the profile likelihood $\chi^2(\theta)$. The procedure ensures the minimum of $\chi^2(\theta)$ appears at the same value as the MLE, avoiding the potential volume effects mentioned in the introduction.

A confidence region, which has the correct frequentist coverage properties, can then be extracted from the likelihood ratio statistic, or equivalently the $\Delta\chi^2(\theta) = \chi^2(\theta) - \chi^2_{\rm min}$ distribution. For a parabolic $\chi^2(\theta)$ shape (i.e. Gaussian estimator distribution), a $1 - \alpha$ level confidence interval is obtained by the set of values $\Delta\chi^2(\theta) \leq \chi^2_1(\alpha)$, where $\chi^2_1(\alpha)$ denotes the $1 - \alpha$ quantile of the chi-square distribution with one degree of freedom, and is 1, 2.7, and 3.84 for $1 - \alpha = 68,\ 90$ and 95% respectively (e.g., James 2007).

It is less well known that if the profile likelihood is non-parabolic, one can still build an approximate confidence interval using the same recipe, because the full likelihood ratio has the invariance property mentioned in the introduction: one can estimate any monotonic function of θ and make the same inference not only on the MLE but on any likelihood ratio. For example,

---

[4] Available from http://seal.web.cern.ch/seal/work-packages/mathlibs/minuit/index.html

[5] As discussed in http://seal.cern.ch/documents/minuit/mnerror.pdf

one can build the $\Delta\chi^2(A_s)$ distribution from the $\Delta\chi^2(\ln(10^{10}A_s))$ profile by simply switching the $\ln(10^{10}A_s) \rightarrow A_s$ axis. Formally, when the profile likelihood is non-parabolic, one can still imagine a transformation that would make it quadratic in the new variable. One would then apply the parabolic cuts described previously and, by the invariance property, the same inference on the original variable would be obtained. Therefore we can find an (asymmetric) confidence interval by cutting the non-parabolic $\Delta\chi^2$ curve at the same $\chi^2(\alpha)$ values. This method, sometimes called `MINOS` (the name of the routine that first implemented it in `Minuit`), is long known in the statistics field (Wilks 1938). It is exact up to order $O(1/N)$ (James 2007), N being the number of samples, and is in practice excellent unless N is very small.

Nevertheless, the profile-likelihood-based confidence intervals must be revisited in the case where the estimate lies near a physical boundary. This will be performed in Sect. 4.2 for the neutrino mass case.

3. Data sets

As our purpose is to compare the frequentist methodology to the Bayesian one, we focus on exactly the same data and parameters as in Planck Collaboration XVI (2014) and refer the reader to Planck Collaboration XV (2014) for their exact definitions. Since the CMB, baryon acoustic oscillation (BAO), and CMB-lensing data were found to be in excellent agreement, we will consider the following likelihood combinations.

The CMB data set consists of the following likelihoods:

- the *Planck* 2013 data in both low and high ℓ ranges;
- the WMAP low-ℓ polarization data (referred to as WP in the *Planck* papers);
- the SPT (Reichardt et al. 2012)+ACT (Das et al. 2014) high-ℓ data, referred to as highL.

The combined likelihood, obtained by multiplying the three, includes 31 nuisance parameters, related to the characterization of the unresolved foregrounds, the effective beam, and to the intercalibration of the *Planck* and highL power spectra.

The BAO data set consists of a Gaussian likelihood based on the scale measurements from the 6dF (Beutler et al. 2011), SDSS (Padmanabhan et al. 2012), and BOSS (Anderson et al. 2012) experiments, combined as in Planck Collaboration XVI (2014).

For the neutrino mass case, we will also use the *Planck* lensing likelihood (Planck Collaboration XVII 2014), based on the measurement of the deflection power spectrum.

4. Results

4.1. The base ΛCDM model

We begin by revisiting the global best-fit solution (MLE) using this new minimizer, over all 37 parameters, on the CMB and CMB+BAO data sets. We use the Hubble constant (H_0) instead of the CMB acoustic scale (θ_{MC}), which is not available within `class`, and z_{re} instead of τ since it is more stable as discussed in Sect. 2.1. The new minimum is given in Table 3 and compared to the results previously released in Planck Collaboration XVI (2014), which were obtained with another minimizer[6]. In both cases we find a slightly lower χ^2. On the cosmological side we find very similar parameters, except for z_{re} which is slightly

shifted. On the nuisance parameters side, results are also similar, but we are now sensitive to the SZ–CIB cross-correlation parameter $\xi^{tSZ-CIB}$ while the Planck Collaboration minimum was not shifted from its zero initial value. Additionally the estimated kinetic SZ amplitude A^{kSZ} is more stable when including the BAO data set.

We then build the profile likelihoods by scanning each cosmological parameter and computing the χ^2 minimum in the remaining 36 dimensions at each point. Figure 2 shows the reconstructed profiles. They are found to be mostly parabolic, but we still fit them with a third-order polynomial in order to measure any deviation from a symmetric error, and threshold them at unity in order to obtain the 68% frequentist confidence level interval as explained in Sect. 2.3. Results are reported in Table 4 and compared there to the Planck Collaboration posterior distributions. In most cases the values and errors we obtain are in good agreement with the Bayesian posteriors, demonstrating that the Planck Collaboration results, for the ΛCDM model, are not biased by a particular choice of parameters (implicit priors) or by the marginalization process (volume effects).

By comparing the mean values of Table 4 to the best-fit ones (Table 3) we observe that the minima coincide at the percent level, as expected for this frequentist method.

Since we observe some difference in the reionization parameter z_{re}, we also perform the profile-likelihood analysis with the *Planck* data alone and obtain

$$z_{re} = 13.3^{+2.8}_{-3.3} \qquad (Planck\text{-}only, \text{profile likelihood}), \qquad (1)$$

while the Planck Collaboration reports

$$z_{re} = 11.4^{+4.0}_{-2.8} \qquad (Planck\text{-}only, \text{MCMC posterior}). \qquad (2)$$

The results, using exactly the same data, are different. We believe that these new results are robust since the profile-likelihood method is particularly well suited for this case. Indeed z_{re} is fixed in each step so that the minimization does not suffer from the classical (A_s, z_{re}) degeneracy due to the normalization of the temperature-only power spectrum. In contrast, the MCMC method relies strongly on the priors used on both A_s and z_{re}. We find that it is the inclusion of the WMAP polarization data that pulls down this value to $z_{re} = 11.0 \pm 1.1$, as reported in Table 4.

4.2. Mass of standard neutrinos

Since the cosmological parameter posterior distributions for the ΛCDM model are mostly Gaussian (parabolic χ^2), the Bayesian and frequentist approaches lead to similar results. However, we may expect greater differences when including neutrino masses in the model, for which the marginalized posterior distribution is peaked towards zero.

CMB measurements are sensitive to the sum of neutrino mass eigenstates $\sum m_\nu$ through several effects reviewed in detail in Lesgourgues et al. (2013). For large values $\sum m_\nu \gtrsim 1.3$ eV, the neutrinos' non-relativistic transition happens before decoupling and the integrated Sachs–Wolfe effect reduces the amplitude of the first acoustic peak. For lower mass values, neutrino free-streaming erases small-scale matter fluctuations and accordingly reduces the CMB lensing power. This in turn affects the lensed C_ℓ spectrum, especially its high-ℓ part, and explains the gain when including SPT/ACT data. Furthermore, since according to oscillation experiments at least two neutrinos are non-relativistic today (Beringer et al. 2012), the matter–radiation equality scale factor, which is strongly constrained by the *Planck* data, reads:

$$\frac{a_{eq}}{a_0} = \frac{\omega_r}{\omega_m - \omega_\nu}, \qquad (3)$$

---

[6] Named `BOBYQUA` and described in http://www.damtp.cam.ac.uk/user/na/NA_papers/NA2009_06.pdf

Table 3. Best-fit comparison.

Parameter	CMB		CMB+BAO	
	CosmoMC	Minuit	CosmoMC	Minuit
H_0	67.15	67.28	67.77	67.71
$100\Omega_b h^2$	2.207	2.210	2.216	2.216
$\Omega_c h^2$	0.1203	0.1200	0.1189	0.1190
n_s	0.9582	0.9576	0.9611	0.9600
$\ln(10^{10} A_s)$	3.096	3.087	3.097	3.090
z_{re}	11.37	11.04	11.52	11.26
A_{100}^{PS}	209	207	204	205
A_{143}^{PS}	72.6	73.5	71.8	73.0
A_{217}^{PS}	59.5	61.1	59.4	60.7
A_{143}^{CIB}	3.57	3.03	3.30	3.06
A_{217}^{CIB}	53.9	51.2	53.0	51.2
A_{143}^{tSZ}	5.17	4.00	4.86	4.01
$r_{143\times217}^{PS}$	0.825	0.815	0.824	0.814
$r_{143\times217}^{CIB}$	1.	1.	1.	1.
γ^{CIB}	0.674	0.647	0.667	0.647
c_{100}	1.	1.	1.	1.
c_{217}	0.997	0.997	0.997	0.997
$\xi^{tSZ-CIB}$	0.000	0.049	0.000	0.055
A^{kSZ}	0.89	2.87	1.58	2.89
β_1^1	0.56	0.41	0.46	0.38
$A_{148}^{PS,ACT}$	10.2	10.4	10.2	10.4
$A_{218}^{PS,ACT}$	75.2	76.5	75.6	76.6
$A_{95}^{PS,SPT}$	7.02	7.49	7.14	7.47
$A_{150}^{PS,SPT}$	9.66	9.90	9.76	9.92
$A_{220}^{PS,SPT}$	72.0	73.5	72.6	73.6
$r_{95\times150}^{PS}$	0.830	0.787	0.806	0.790
$r_{95\times220}^{PS}$	0.583	0.545	0.563	0.549
$r_{150\times220}^{PS}$	0.908	0.915	0.911	0.915
A_{dust}^{ACTs}	0.429	0.426	0.429	0.426
A_{dust}^{ACTe}	0.879	0.845	0.843	0.844
y_{ACTs}^{148}	0.991	0.991	0.992	0.991
y_{ACTs}^{217}	1.	1.	1.	1.
y_{ACTe}^{148}	0.987	0.987	0.988	0.988
y_{ACTe}^{217}	0.960	0.961	0.961	0.962
y_{SPT}^{95}	0.985	0.983	0.985	0.983
y_{SPT}^{150}	0.984	0.984	0.985	0.985
y_{SPT}^{220}	1.02	1.02	1.02	1.02
χ_{min}^2	10 509.9	10 508.9	10 511.0	10 510.3

Notes. Values of all parameters at the minimum of the χ^2 function as determined by `CosmoMC` in Planck Collaboration XVI (2014) and by the `Minuit` implementation described here, for the CMB and CMB+BAO data sets. The first six parameters define the ΛCDM cosmology. The last line shows the χ^2 value at the minimum.
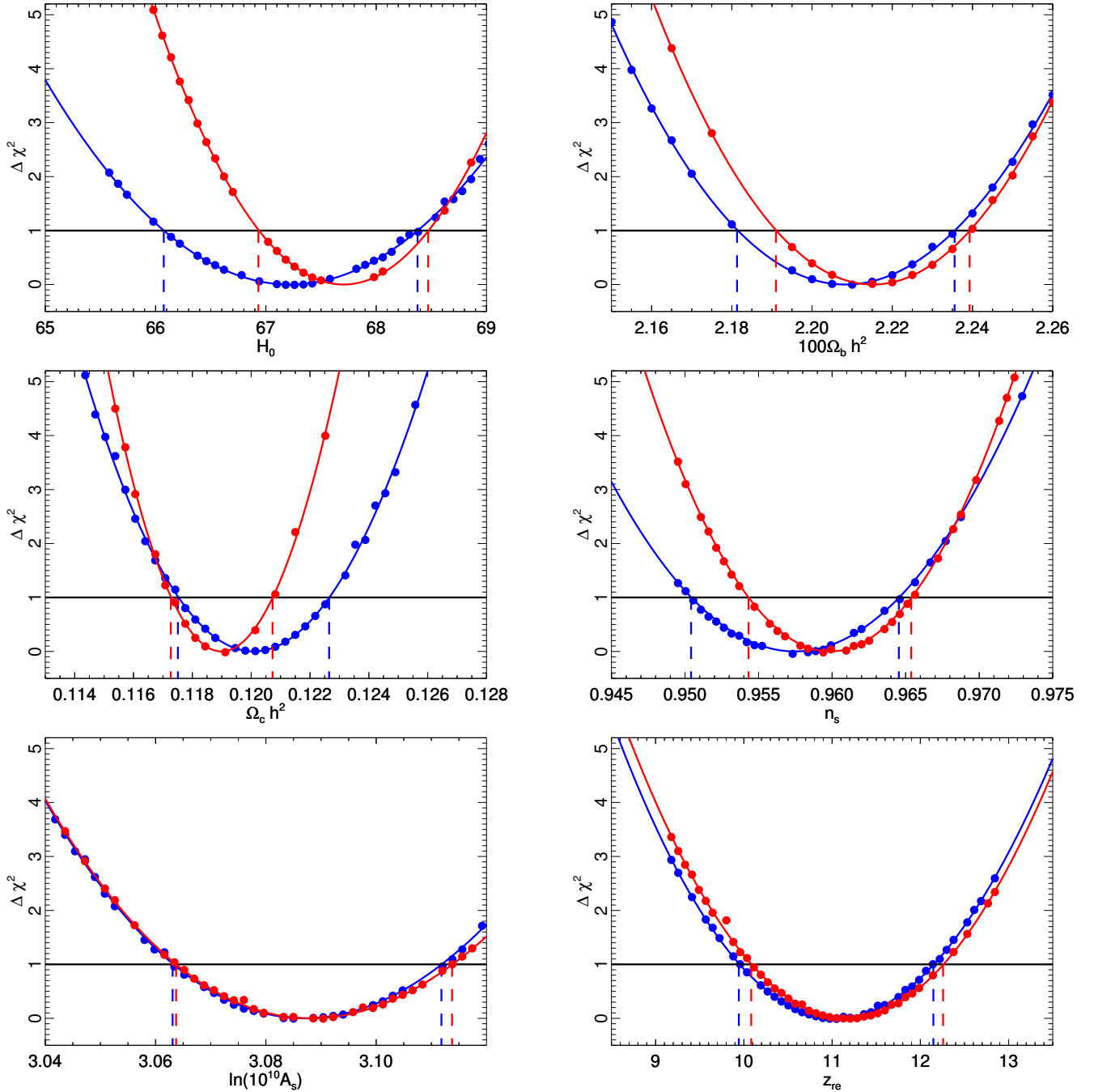
Fig. 2. Profile likelihoods ($\Delta\chi^2$) reconstructed for each ΛCDM cosmological parameter, from the CMB (blue) and CMB+BAO (red) data sets. Each point is the result of a 36-parameter minimization. We reject the points that are outliers of the expected distance to minimum (EDM, Sect. 2.2) distribution. Curves are fits to a third-order polynomial. 68% confidence intervals are obtained by thresholding these curves at unity, and their projections onto the parameter axis are shown.

Table 4. Results of the profile-likelihood analysis (i.e., this work) for the cosmological parameters, using the CMB and CMB+BAO data sets.

Parameter	CMB				CMB+BAO			
	MCMC		Profile-likelihood		MCMC		Profile-likelihood	
H_0	67.3	± 1.2	67.2	± 1.2	67.8	± 0.8	67.7	± 0.8
$100\omega_b$	2.207	± 0.027	2.208	± 0.027	2.214	± 0.024	2.215	± 0.024
ω_c	0.1198	± 0.0026	0.1201	± 0.0026	0.1187	± 0.0017	0.1190	± 0.0017
n_s	0.9585	± 0.0070	0.9575	± 0.0071	0.9608	± 0.0054	0.9598	± 0.0055
$\ln(10^{10}A_s)$	3.090	± 0.025	3.087	± 0.025	3.091	± 0.025	3.088	± 0.025
z_{re}	11.2	± 1.1	11.0	± 1.1	11.2	± 1.1	11.2	± 1.1

Notes. They are compared to the *Planck* MCMC posterior results taken from Table 5 of Planck Collaboration XVI (2014).
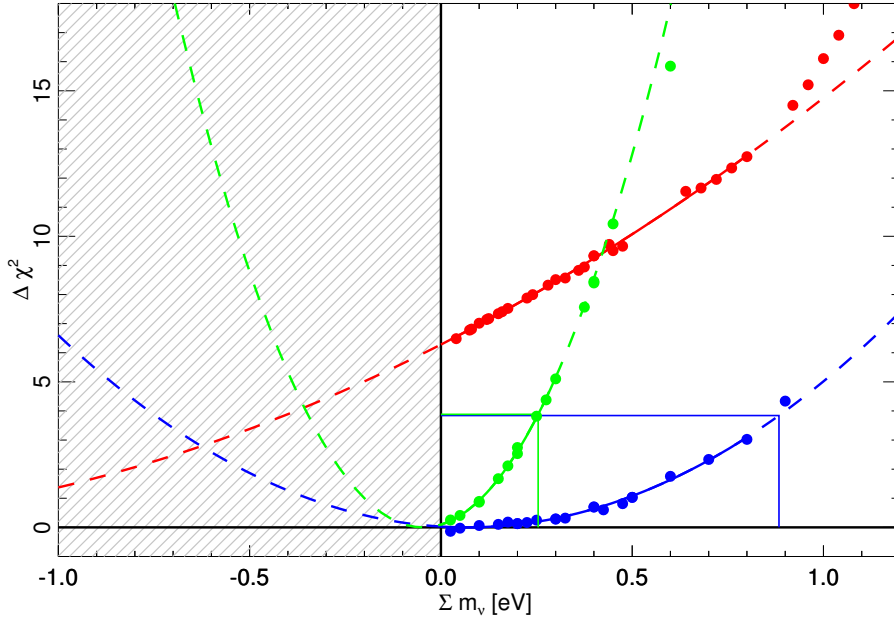
Fig. 3. Neutrino mass profile likelihood for the CMB (red), CMB+lensing (blue), and CMB+lensing+BAO (green) data sets. Each point is the result of a 37-parameter fit which can only be computed in the positive region. The points are fit by a parabola and extrapolated into the negative region. For the CMB only case, the parabolic fit agreement is poor and is only shown for discussion. The coloured green/blue lines are used to set 95% confidence upper limits according to the Feldman-Cousins prescription, as described in the text.

where ω_r, ω_m, and ω_ν are the physical densities of radiation, matter, and massive neutrinos respectively, i.e. $\omega_r = \Omega_r h^2$, $\omega_m = \Omega_m h^2$, and $\omega_\nu = \Omega_\nu h^2 \simeq 10^{-3} \sum m_\nu / 0.1$ eV. The quantities ω_ν and ω_m are clearly degenerate, and so any data set that helps in reducing the CMB geometrical degeneracies by providing a measurement at another scale indirectly benefits $\sum m_\nu$. Robust observables, compatible with the *Planck* ΛCDM cosmology, are the BAO scale measurement around $z \simeq 0.5$ and/or the CMB-lensing trispectrum that probes matter structures around $z \simeq 2$.

An unexpected result found by Planck Collaboration XVI (2014) is that the 95% confidence upper limit on $\sum m_\nu$ obtained from *Planck* data is worsened when including the lensing trispectrum information (the 95% upper limit goes from 0.66 to 0.84). How can the addition of new information weaken the limit? Is this an effect of the Bayesian methodology, which computes credible intervals and where such effects may arise when combining incompatible data? Naively, in a frequentist analysis adding some information (in the Fisher sense, see James 2007) can only lower the size of confidence interval, since the profile-likelihood "error" (its curvature at the minimum) can only decrease and thresholding it at a constant value should only lead to a smaller region.

We construct the profile likelihood for $\sum m_\nu$. It is shown in Fig. 3 for the CMB, CMB+lensing and CMB+lensing+BAO data sets. We observe an intriguing feature with the CMB data set. Even though the parabolic fit of the profile likelihood is poor, the minimum lies at about -2.5σ into the unphysical negative region. When adding the lensing trispectrum information, it shifts back to a value compatible with zero. We do not yet have a proper understanding of why this is happening, but note a possible connection to the A_L issue discussed in Planck Collaboration XVI (2014), where this phenomenological parameter is discrepant from unity by about 2σ using the CMB data set, but lowered to 1σ when adding the lensing information.

We can then understand why our previous argument on reducing the confidence interval by adding information is invalid near a physical boundary, even in a frequentist sense. If we consider a constant threshold of the profile likelihood (for instance around 8 in Fig. 3) we may end up with an upper limit that is smaller (even though the curvature is larger) when omitting the

Table 5. Estimates of the minima positions (m_0) and curvature (σ_ν) from the parabolic fits of Fig. 3 for the data sets including lensing.

Data set	Fitted range	m_0	σ_ν
CMB+lensing	[0, 0.8]	0.06	0.42
CMB+lensing+BAO	[0, 0.3]	−0.05	0.15

Notes. The range of points used corresponds roughly to 2σ.

lensing information, because of the shift of the minimum into the unphysical region. This resembles the Bayesian result.

However the methodologies shows their differences in this situation. In the Bayesian case, when combining somewhat incompatible data sets within a model the credible region enlarges to account for it. In the frequentist case, thresholding the profile likelihood is incorrect and we apply instead the Feldman & Cousins (1998) prescription. Within this classical framework, there is a decoupling of the confidence level of the goodness of fit probability from the one used in building the confidence interval. Unlike in the Bayesian case, one first tests the consistency of the data with the model, and then constructs the confidence interval (at some given level) only for the candidates that fulfil it. In our case, a minimum at -2.5σ is very unlikely (below 1% probability) and we will therefore not consider it in the following.

We give in Table 5 the parameters of the parabolic fits $\chi^2(\sum m_\nu) = \chi^2_{min} + [(\sum m_\nu - m_0)/\sigma_\nu]^2$. We only use points within $2\sigma_\nu$ from zero, since the function is not necessarily quadratic far from its minimum. In the following we will vary this cut. We report here the numbers that lead to the largest final limit.

The classical Neyman construction of a confidence interval has some inherent degree of freedom in it (e.g., Beringer et al. 2012). The Feldman–Cousins prescription, that is most powerfull near a physical a boundary, is to introduce an ordering based upon the likelihood ratios R:

$$R = \frac{\mathcal{L}(x|\mu)}{\mathcal{L}(x|\mu_{best})}, \tag{4}$$

Table 6. Upper limit (95% confidence) on the neutrino mass (in eV) in the *Planck* Bayesian framework and in the frequentist one based on Feldman–Cousins prescription.

Data set	Bayesian posterior	Profile likelihood
CMB+lensing	0.85	0.88
CMB+lensing+BAO	0.25	0.26

where x is the measured value of the sum of neutrino masses $\sum m_\nu$, μ is the true value, and μ_{best} is the best-fit value of $\sum m_\nu$, given the data and the physically-allowed region for μ. Hence we have $\mu_{\text{best}} = x$ if $x \geq 0$, but $\mu_{\text{best}} = 0$ if $x < 0$, and the ratio R is given by (Feldman & Cousins 1998):

$$\exp(-(x-\mu)^2/2) \quad \text{for } x > 0, \tag{5}$$

$$\exp(x\mu - \mu^2/2) \quad \text{for } x \leq 0. \tag{6}$$

We then search for an interval $[x_1, x_2]$ such that $R(x_1) = R(x_2)$ and

$$\int_{x_1}^{x_2} \mathcal{L}(x|\mu)\mathrm{d}x = \alpha, \tag{7}$$

with $\alpha = 0.95$ as the confidence level. These intervals are tabulated in Feldman & Cousins (1998).

We obtain the confidence interval $[\mu_1, \mu_2]$ for each $x = m_0/\sigma_\nu$ extracted from the parabolic fit to the χ^2 profile as given in Table 5. The upper limits are then simply $\mu_2 \times \sigma_\nu$.

We give our final results in Table 6 and compare them to the *Planck* Bayesian ones of Planck Collaboration XVI (2014). The agreement is impressive, despite the use of two very different statistical techniques. Finally, we varied the range of points used in the parabolic fit and the limits we obtain are always lower than the one reported in Table 6, meaning that our results are conservative.

5. Conclusion

The use of Bayesian methodology in cosmology is partly motivated by the fact that one observes a single realization of the Universe, while, in particle physics, one accumulates a number of events which leads more naturally to using frequentist methods. This argument is of a sociological rather than scientific nature, and nothing prevents us from using one or the other methodology in these fields.

We demonstrated that a purely frequentist method is tractable with the recent *Planck*-led high-precision cosmology data. It required lowering the numerical noise of the Boltzmann solver code and we have provided a set of precision parameters for the `class` software that, in conjunction with a proper `Minuit` minimization strategy, allowed us to perform the roughly 40 parameter optimization efficiently. We re-determined the maximum likelihood solution, obtaining essentially consistent results but with a slightly better χ^2 value.

We built profile likelihoods for each of the cosmological parameters of the ΛCDM model, using the CMB and CMB+BAO data sets, and obtained results very similar to those from the Bayesian methodology. This confirmed, in this model, that the *Planck* results do not depend on the choice of base parameters (implicit priors) and are free of volume effects in the likelihood projection during the marginalization process.

When including the neutrino mass as a free parameter, the profile likelihood helped us to understand why the computed upper limit increases when including the extra information from CMB lensing. This is not due to the Bayesian methodology, but is related to the physical boundary $\sum m_\nu > 0$. The profile likelihood analysis showed that neutrino mass limits obtained without using the lensing information were pulled down to unphysical negative values. Including the extra CMB lensing information allowed us to obtain consistent frequentist results.

Using the Feldman–Cousins prescription, we obtained a 95% confidence upper limit of $\sum m_\nu \leq 0.26$ eV for the CMB+lensing+BAO combination, again in excellent agreement with the Bayesian result.

Appendix A: Note on CPU time

It it sometimes stated that multi-dimensional minimization in high-dimension space is inefficient (or intractable) while MCMC methods scale linearly. Both statements need clarification.

Standard MCMC methods (e.g., Metropolis–Hastings or Gibbs sampling as in `CosmoMC`) are extremely CPU-intensive. They require the lengthy computation of a multi-variate proposal before running a final Markov chain, which by essence is sequential and therefore cannot scale on multiple processors. In the *Planck* case about $O(10^5)$ iterations (i.e., computations of the likelihood) were needed for this final stage.

One `Minuit` minimization in our scheme is obtained in about $O(10^4)$ iterations. It, however, requires a higher precision tuning of the Boltzmann solver, which enhances the computation time of each likelihood by about a factor two. In practice the minimum, in the $D = 40$ case, is found in about 10 h, and is limited by the Boltzmann computation speed. The profile likelihood approach requires many minimizations but these are independent of one another. The problem now scales with the number of computers, so that the total wall-clock time is still of the same order of magnitude on a reasonable computer cluster.

References

Anderson, L., Aubourg, E., Bailey, S., et al. 2012, MNRAS, 427, 3435
ATLAS Collaboration. 2013, Combined measurements of the mass and signal strength of the Higgs-like boson with the ATLAS detector using up to 25 fb^{-1} of proton-proton collision data, Tech. Rep. ATLAS-CONF-2013-014, CERN, Geneva
Beringer, J., Arguin, J. F., Barnett, R. M., et al. 2012, Phys. Rev. D, 86, 010001
Beutler, F., Blake, C., Colless, M., et al. 2011, MNRAS, 416, 3017
Blas, D., Lesgourgues, J., & Tram, T. 2011, J. Cosmol. Astropart. Phys., 7, 34
Christensen, N., Meyer, R., Knox, L., & Luey, B. 2001, Class. Quant. Grav., 18, 2677
Das, S., Louis, T., Nolta, M. R., et al. 2014, JCAP, 04, 014
Davidon, W., & Laboratory, A. N. 1959, Variable metric method for minimization, AEC research and development report (Argonne National Laboratory)
Feldman, G. J., & Cousins, R. D. 1998, Phys. Rev. D, 57, 3873
Fletcher, R. 1970, Comput. J., 317

Gonzalez-Morales, A. X., Poltis, R., Sherwin, B. D., & Verde, L. 2011, unpublished [arXiv:1106.5052]

Hamann, J. 2012, J. Cosmol. Astropart., 3, 21

Hamann, J., Hannestad, S., Raffelt, G. G., & Wong, Y. Y. Y. 2007, J. Cosmol. Astropart. Phys., 8, 21

James, F. 2007, Statistical Methods in Experimental Physics (World Scientific)

James, F., & Roos, M. 1975, Comput. Phys. Commun., 10, 343

Kosowsky, A., Milosavljevic, M., & Jimenez, R. 2002, Phys. Rev. D, 66, 063007

Lesgourgues, J. 2011a, unpublished [arXiv:1104.2932]

Lesgourgues, J. 2011b, unpublished [arXiv:1104.2934]

Lesgourgues, J., Mangano, G., Miele, G., & Pastor, S. 2013, Neutrino Cosmology (Cambridge: Cambridge Univ. Press)

Lewis, A. 2008, Phys. Rev. D, 78, 023002

Lewis, A., & Bridle, S. 2002, Phys. Rev. D, 66, 103511

Padmanabhan, N., Xu, X., Eisenstein, D. J., et al. 2012, MNRAS, 427, 2132

Planck Collaboration I. 2014, A&A, in press, DOI: 10.1051/0004-6361/201321529

Planck Collaboration XV. 2014, A&A, in press, DOI: 10.1051/004-6361/201321573

Planck Collaboration XVI. 2014, A&A, in press, DOI: 10.1051/0004-6361/201321591

Planck Collaboration XVII. 2014, A&A, in press, DOI: 10.1051/0004-6361/201321543

Reichardt, C. L., de Putter, R., Zahn, O., & Hou, Z. 2012, ApJ, 749, L9

Reid, B. A., Verde, L., Jimenez, R., & Mena, O. 2010, J. Cosmol. Astropart. Phys., 1, 3

Wilks, A. S. S. 1938, Ann. Math. Statist., 1, 60

Yèche, C., Ealet, A., Réfrégier, A., et al. 2006, A&A, 448, 831

[1] APC, AstroParticule et Cosmologie, Université Paris Diderot, CNRS/IN2P3, CEA/lrfu, Observatoire de Paris, Sorbonne Paris Cité, 10 rue Alice Domon et Léonie Duquet, 75205 Paris Cedex 13, France

[2] Aalto University Metsähovi Radio Observatory and Dept of Radio Science and Engineering, PO Box 13000, 00076 Aalto, Finland

[3] African Institute for Mathematical Sciences, 6-8 Melrose Road, Muizenberg, Cape Town, South Africa

[4] Agenzia Spaziale Italiana Science Data Center, via del Politecnico snc, 00133 Roma, Italy

[5] Agenzia Spaziale Italiana, Viale Liegi 26, Roma, Italy

[6] Astrophysics Group, Cavendish Laboratory, University of Cambridge, J J Thomson Avenue, Cambridge CB3 0HE, UK

[7] Astrophysics & Cosmology Research Unit, School of Mathematics, Statistics & Computer Science, University of KwaZulu-Natal, Westville Campus, Private Bag X54001, 4000 Durban, South Africa

[8] Atacama Large Millimeter/submillimeter Array, ALMA Santiago Central Offices, Alonso de Cordova 3107, Vitacura, Casilla 763 0355, Santiago, Chile

[9] CITA, University of Toronto, 60 St. George St., Toronto, ON M5S 3H8, Canada

[10] CNRS, IRAP, 9 Av. colonel Roche, BP 44346, 31028 Toulouse Cedex 4, France

[11] California Institute of Technology, Pasadena, California, USA

[12] Centro de Estudios de Física del Cosmos de Aragón (CEFCA), Plaza San Juan 1, planta 2, 44001 Teruel, Spain

[13] Computational Cosmology Center, Lawrence Berkeley National Laboratory, Berkeley, California, USA

[14] Consejo Superior de Investigaciones Científicas (CSIC), Madrid, Spain

[15] DSM/Irfu/SPP, CEA-Saclay, 91191 Gif-sur-Yvette Cedex, France

[16] DTU Space, National Space Institute, Technical University of Denmark, Elektrovej 327, 2800 Kgs. Lyngby, Denmark

[17] Département de Physique Théorique, Université de Genève, 24 Quai E. Ansermet, 1211 Genève 4, Switzerland

[18] Departamento de Física, Universidad de Oviedo, Avda. Calvo Sotelo s/n, Oviedo, Spain

[19] Department of Astrophysics/IMAPP, Radboud University Nijmegen, PO Box 9010, 6500 GL Nijmegen, The Netherlands

[20] Department of Physics and Astronomy, Dana and David Dornsife College of Letter, Arts and Sciences, University of Southern California, Los Angeles CA 90089, USA

[21] Department of Physics and Astronomy, University College London, London WC1E 6BT, UK

[22] Department of Physics and Astronomy, University of Sussex, Brighton BN1 9QH, UK

[23] Department of Physics, Florida State University, Keen Physics Building, 77 Chieftan Way, Tallahassee, Florida, USA

[24] Department of Physics, Gustaf Hällströmin katu 2a, University of Helsinki, Helsinki, Finland

[25] Department of Physics, Princeton University, Princeton, New Jersey, USA

[26] Department of Physics, University of California, Berkeley, California, USA

[27] Department of Physics, University of California, One Shields Avenue, Davis, California, USA

[28] Department of Physics, University of California, Santa Barbara, California, USA

[29] Department of Physics, University of Illinois at Urbana-Champaign, 1110 West Green Street, Urbana, Illinois, USA

[30] Dipartimento di Fisica e Astronomia G. Galilei, Università degli Studi di Padova, via Marzolo 8, 35131 Padova, Italy

[31] Dipartimento di Fisica e Scienze della Terra, Università di Ferrara, via Saragat 1, 44122 Ferrara, Italy

[32] Dipartimento di Fisica, Università La Sapienza, P.le A. Moro 2, Roma, Italy

[33] Dipartimento di Fisica, Università degli Studi di Milano, via Celoria, 16, Milano, Italy

[34] Dipartimento di Fisica, Università degli Studi di Trieste, via A. Valerio 2, Trieste, Italy

[35] Dipartimento di Fisica, Università di Roma Tor Vergata, via della Ricerca Scientifica 1, Roma, Italy

[36] Discovery Center, Niels Bohr Institute, Blegdamsvej 17, Copenhagen, Denmark

[37] Dpto. Astrofísica, Universidad de La Laguna (ULL), 38206 La Laguna, Tenerife, Spain

[38] European Southern Observatory, ESO Vitacura, Alonso de Cordova 3107, Vitacura, Casilla 19001, Santiago, Chile

[39] European Space Agency, ESAC, Planck Science Office, Camino bajo del Castillo s/n, Urbanización Villafranca del Castillo, Villanueva de la Cañada, Madrid, Spain

[40] European Space Agency, ESTEC, Keplerlaan 1, 2201 AZ Noordwijk, The Netherlands

[41] Helsinki Institute of Physics, Gustaf Hällströmin katu 2, University of Helsinki, Helsinki, Finland

[42] INAF – Osservatorio Astrofisico di Catania, via S. Sofia 78, Catania, Italy

[43] INAF – Osservatorio Astronomico di Padova, Vicolo dell'Osservatorio 5, Padova, Italy

[44] INAF – Osservatorio Astronomico di Roma, via di Frascati 33, Monte Porzio Catone, Italy

[45] INAF – Osservatorio Astronomico di Trieste, via G.B. Tiepolo 11, Trieste, Italy

[46] INAF Istituto di Radioastronomia, via P. Gobetti 101, 40129 Bologna, Italy

[47] INAF/IASF Bologna, via Gobetti 101, Bologna, Italy

[48] INAF/IASF Milano, via E. Bassini 15, Milano, Italy

[49] INFN, Sezione di Bologna, via Irnerio 46, 40126, Bologna, Italy

[50] INFN, Sezione di Roma 1, Università di Roma Sapienza, Piazzale Aldo Moro 2, 00185 Roma, Italy

[51] INFN/National Institute for Nuclear Physics, via Valerio 2, 34127 Trieste, Italy

[52] IUCAA, Post Bag 4, Ganeshkhind, Pune University Campus, 411 007 Pune, India

[53] Imperial College London, Astrophysics group, Blackett Laboratory, Prince Consort Road, London, SW7 2AZ, UK

[54] Infrared Processing and Analysis Center, California Institute of Technology, Pasadena CA 91125, USA

[55] Institut Universitaire de France, 103 bd Saint-Michel, 75005 Paris, France

[56] Institut d'Astrophysique Spatiale, CNRS (UMR 8617) Université Paris-Sud 11, Bâtiment 121, Orsay, France

[57] Institut d'Astrophysique de Paris, CNRS (UMR 7095), 98bis Boulevard Arago, 75014 Paris, France

[58] Institute for Space Sciences, Bucharest-Magurale, Romania

[59] Institute of Astronomy, University of Cambridge, Madingley Road, Cambridge CB3 0HA, UK

[60] Institute of Theoretical Astrophysics, University of Oslo, Blindern, Oslo, Norway

[61] Instituto de Astrofísica de Canarias, C/Vía Láctea s/n, La Laguna, Tenerife, Spain

[62] Instituto de Física de Cantabria (CSIC-Universidad de Cantabria), Avda. de los Castros s/n, Santander, Spain

[63] Jet Propulsion Laboratory, California Institute of Technology, 4800 Oak Grove Drive, Pasadena, California, USA

[64] Jodrell Bank Centre for Astrophysics, Alan Turing Building, School of Physics and Astronomy, The University of Manchester, Oxford Road, Manchester, M13 9PL, UK

[65] Kavli Institute for Cosmology Cambridge, Madingley Road, Cambridge, CB3 0HA, UK

[66] LAL, Université Paris-Sud, CNRS/IN2P3, Orsay, France

[67] LERMA, CNRS, Observatoire de Paris, 61 Avenue de l'Observatoire, Paris, France

[68] Laboratoire AIM, IRFU/Service d'Astrophysique – CEA/DSM – CNRS – Université Paris Diderot, Bât. 709, CEA-Saclay, 91191 Gif-sur-Yvette Cedex, France

[69] Laboratoire Traitement et Communication de l'Information, CNRS (UMR 5141) and Télécom ParisTech, 46 rue Barrault, 75634 Paris Cedex 13, France

[70] Laboratoire de Physique Subatomique et de Cosmologie, Université Joseph Fourier Grenoble I, CNRS/IN2P3, Institut National Polytechnique de Grenoble, 53 rue des Martyrs, 38026 Grenoble Cedex, France

[71] Laboratoire de Physique Théorique, Université Paris-Sud 11 & CNRS, Bâtiment 210, 91405 Orsay, France

[72] Lawrence Berkeley National Laboratory, Berkeley, California, USA

[73] Max-Planck-Institut für Astrophysik, Karl-Schwarzschild-Str. 1, 85741 Garching, Germany

[74] National University of Ireland, Department of Experimental Physics, Maynooth, Co. Kildare, Ireland

[75] Niels Bohr Institute, Blegdamsvej 17, Copenhagen, Denmark

[76] Optical Science Laboratory, University College London, Gower Street, London, UK

[77] SISSA, Astrophysics Sector, via Bonomea 265, 34136 Trieste, Italy

[78] SUPA, Institute for Astronomy, University of Edinburgh, Royal Observatory, Blackford Hill, Edinburgh EH9 3HJ, UK

[79] School of Physics and Astronomy, Cardiff University, Queens Buildings, The Parade, Cardiff, CF24 3AA, UK

[80] UPMC Univ. Paris 06, UMR 7095, 98bis Boulevard Arago, 75014 Paris, France

[81] Université de Toulouse, UPS-OMP, IRAP, 31028 Toulouse Cedex 4, France

[82] University of Granada, Departamento de Física Teórica y del Cosmos, Facultad de Ciencias, Granada, Spain

[83] University of Granada, Instituto Carlos I de Física Teórica y Computacional, Granada, Spain

[84] Warsaw University Observatory, Aleje Ujazdowskie 4, 00-478 Warszawa, Poland